Crystal structure of cobalt molybdate hydrate CoMoO4・nH2O

Eda, Kazuo
Uno, Yuichi
Nagai, Noriko
Sotani, Noriyuki
Whittingham, M. Stanley

(Citation)
Journal of Solid State Chemistry,178(9):2791-2797

(Issue Date)
2005-09

(Resource Type)
journal article

(Version)
Accepted Manuscript

(URL)
https://hdl.handle.net/20.500.14094/90000965

Kazuo Eda,
Department of Chemistry, Faculty of Science, Kobe University, Nada-ku, Kobe 657-8501, Japan
Tel: +81-78-803-5677, Fax: +81-78-803-5677, E-mail: eda@kobe-u.ac.jp

Crystal Structure of Cobalt Molybdate Hydrate $CoMoO_4 \cdot nH_2O$

Kazuo Eda,*[a] Yuichi Uno,[a] Noriko Nagai,[a] Noriyuki Sotani,[a] M. Stanley Whittingham[b]

[a]*Department of Chemistry, Faculty of Science, Kobe University, Nada-ku, Kobe 657-8501, Japan.*
[b]*Institute for Materials Research, State University of New York at Binghamton, Binghamton, NY 13902-6000, U.S.A.*

* To whom correspondence should be addressed

Abstract

We have determined the crystal structure of the title compound, which has a triclinic cell with cell parameters of a=6.844 Å, b=6.933 Å, c=9.339 Å, α=76.617 °, β=84.188 °, γ=74.510 ° and space group $P\bar{1}$. The crystal structure suggests the chemical formula $CoMoO_4 \cdot 3/4H_2O$. The structure consists of MoO_4 tetrahedra and CoO_6 octahedra, confirming the earlier XANES investigation on the hydrate. The comparison of the crystal structures of the hydrate and the α-, β-, and hp-phases shows that the hydrate exhibits metal cation coordinations similar to those of the β-phase, but had arrangements of CoO_6 and MoO_n polyhedra similar to those of the hp-phase.

Key words: crystal structure, cobalt molybdate, oxide hydrate, $CoMoO_4 \cdot nH_2O$

Introduction

Cobalt molybdates are attractive compounds because of their structural, magnetic, and catalytic properties [1-9]. They are especially important components of industrial catalysts. Their catalytic properties are closely related to their structure [5,7]. Four compounds with the $CoMoO_4$ stoichiometry are known: the low temperature α-phase (pale green, space group: $C2/m$; a=9.67, b=8.85, c=7.76 Å, β=113.49 °) [10], the high temperature β-phase (pale violet, $C2/m$; a=10.21, b=9.31, c=7.01 Å, β=106.4 °) [2,11], the high-pressure (hp-) phase (black, $P2/c$, a=4.6598, b=5.6862, c=4.9159 Å, β=90.521 °) [4], and the hydrate (violet, crystal structure: unknown up to now). The hydrate has been known to directly transform into the β-phase when it entirely loses its crystallization water at around 600 K. This transformation occurs at much lower temperature than the transition from α-phase to β-phase (ca. 750), and is probably facilitated by the structural similarities of the hydrate and β-phase [8]. Recently we have found another direct transformation of the hydrate into the hp-phase under hydrothermal conditions, which transformation will be presented elsewhere. In order to understand not only these transformations but also their catalytic or physical properties, comparison of their structures is necessary. The crystal structures of three out of the four compounds (except the hydrate) are known as mentioned above. It is only suggested that the hydrate

consists of CoO_6 and MoO_4 polyhedra according to X-ray absorption near-edge spectroscopic (XANES) investigation [8].

In order to reveal the structure of the hydrate, we succeeded in preparing a single crystal of it. The single crystal analysis confirmed that the hydrate consists of CoO_6 and MoO_4 polyhedra, and the polyhedra in the hydrate are connected similarly to that in the hp-phase rather than those in α– and β-phases. In the present paper we will present the structure of the hydrate and compare it with the structures of the $CoMoO_4$ phases.

Experimental

Preparation of the hydrate: 0.720 g of MoO_3 (5 mmol) and 0.375 g of CoO (5 mmol), were suspended in 30ml of distilled water. 0.292 g of NaCl (5mmol) was added to the solution in order to increase the ionic strength of the solution and promote crystal growth of the hydrate during the hydrothermal treatment. Then the solution was put into a 60 ml Teflon-lined autoclave and heated in a forced convection oven at 453 K under autogenous pressure (ca. 10 atm) for 1 day. The resulting product was filtered, washed with distilled water, and dried in air at room temperature. Even without the addition of NaCl a single phase product of the hydrate was obtained and confirmed by powder X-ray diffraction, but no crystals sufficient for single crystal X-ray analysis were grown in spite of varying treatment temperature (up to 473 K), treatment time, as well as the

concentrations of MoO_3 and CoO.

Crystal structure determination of the hydrate: Single crystal diffraction data were collected on a Bruker smart 1000 diffractometer with a CCD detector using graphite monochromated Mo$K\alpha$ radiation. The structure of the single crystal was solved by direct method and refined by full-matrix least-squares calculations based on F_o^2 with empirical absorption corrections using Bruker SHELXTL programs.

Characterization of the hydrate: Powder X-ray diffraction (XRD) patterns of the samples were measured using a Bruker AXS MXP3VZ X-ray diffractometer with Cu $K\alpha$ radiation. Simulation of the diffraction pattern was calculated using Rietan 2000 [12]. The compositions of the products were analyzed by a HITACHI 180-80 atomic absorption spectrometer. TG-DTA analysis was performed on a Bruker AXS TG-DTA 2010 system at a heating rate of 10 K/min.

Results and discussion

Crystal structures of the hydrate. In order to determine the crystal structure of the hydrate, some crystals obtained were used for collecting diffraction data. All crystals used exhibited non-merohedral twinning, which rotated the reciprocal axes 180 ° about the $a^* + c^*$ axis. Two distinct cell sets were separated using RLATT, identified using SMART (Bruker, 2001) and integrated using SAINT (Bruker, 2001). The combined data

were refined with separate scale factors using SHELXTL. The resulting crystal data and refinement for the hydrate are shown in Table 1. A triclinic cell with cell parameters of a=6.844 Å, b=6.933 Å, c=9.339 Å, α=76.617 °, β=84.188 °, γ=74.510 ° was obtained, which made indexing of the powder diffraction pattern of the hydrate difficult. The powder XRD pattern simulation based on the present crystal data reproduced well the peak positions of the XRD patterns observed for polycrystalline samples of the hydrate obtained in the present work (Fig. 1) and in the literature [8]. Tables 2 and 3 show the atomic parameters and selected interatomic distances respectively. Oxygen atoms were refined with isotropic displacement factors to avoid giving non-positive definite answers. The $O9_{cw}$ is suggested to be an aqua oxygen (coordination water) according to BVS analysis (Table 2). The oxygen atom $O10_{lw}$, which is disordered at two sites around a special position (0.5 0.0 0.5), has no direct connection to other atoms and is regarded to be lattice water. Cavity analysis of the unit cell showed no residual void accessible for solvent, although slightly large peaks (maximum peak: 2.86 eÅ^{-3}, 1.72 Å from O7 and minimum peak: -1.91 eÅ^{-3}, 0.90 Å from O7) remained in the Fourier differential map.

TG-DTA analysis of the hydrate (Fig. 2) suggests that the formula of the hydrate is $CoMoO_4 \cdot 3/4H_2O$ rather than $CoMoO_4 \cdot H_2O$. TG curve shows two kinds of

dehydrations (at 350-450 and 500-620 K) as mentioned in the literature [8]. The former dehydration is reversible, and ascribed to lattice water. The latter is irreversible and accompanied with an exotherm at 610 K, which is superimposed on the broad intrinsic endotherm, shown with an additional one-point dotted line in the figure, due to the desorption. This dehydration leads to the transformation of the hydrate into β-$CoMoO_4$ and was attributed to coordination water. The weight losses of 1.86 and 3.50 % due to the dehydrations correspond to n_{lw}=0.24 and n_{cw}=0.45 respectively, and agree with the formula of $CoMoO_4 \cdot 3/4H_2O$ ($n = n_{lw} + n_{cw} = 3/4$, where $n_{lw} = 0.25$ and $n_{cw} = 0.5$). This suggestion supports the above results, concerning coordination and lattice waters, of single crystal X-ray structure analysis.

Table 3 shows that the hydrate consists of MoO_4 tetrahedra and CoO_6 octahedra, and proves the presence of MoO_4 tetrahedra and CoO_6 octahedra in the hydrate, which has been suggested from XANES investigations [8]. Figure 3 shows a polyhedral representation of the crystal structure of the hydrate, together with the structures of the other three $CoMoO_4$ phases. In the hydrate the lattice water occupies the disordered sites around (0.5 0.0 0.5), as mentioned above, but is omitted in the figure for clarity. According to the figure four CoO_6 octahedra constitute a tetramer (z-shaped) $[CoO_6]_4$ unit sharing edges. The z-shaped $[CoO_6]_4$ units are linked with MoO_4 tetrahedra to form

the three-dimensional oxide network.

The hydrate has a lower density (3.76 g/cm^3) than the α- (4.78 g/cm^3), β- (4.57 g/cm^3) and hp- (5.58 g/cm^3) phases. Thus its unit cell has large cavities, one of which is occupied by the lattice water ($O10_{lw}$). These cavities spread around a line linking the lattice positions (0.5 0.0 0.5) and (0.5 1.0 0.5). Hydrogen atoms of the coordination water ($O9_{cw}$) are projecting into the cavities. Such structural features might be related to its high catalytic activity for hydrosulfurization, compared with other $CoMoO_4$ phases [7,13].

Comparison of the structures. Figure 3 shows that all the four compounds contain CoO_6 octahedra. These octahedra form two types of z-shaped $[CoO_6]_4$ units depending on the compounds, although the units in the hp-phase are not isolated like those in the other three compounds. One is a condensed type of unit that is represented by joining two dimers of edge-shared CoO_6 octahedra with a discrepancy of a half width of the octahedra, which is found in the α- and β- phases (Fig. 3(b) and 3(c)). The other is a lengthened type of unit that is built by joining two dimers with a discrepancy of one and a half width of the octahedra, and is in the hydrate and the hp-phase (Fig. 3(a) and 3(d)). Thus the hydrate exhibits the coordination of Co atom similar to those of the other three phases, and has the further similarity in the connecting manner of the octahedra with the

hp-phase.

As for the MoO_n polyhedra, both tetrahedra (MoO_4) and octahedra (MoO_6) are observed depending on the compound. Octahedra are found in the α- and hp-phases, and are directly linked by sharing edges to form two types of z-shaped $[MoO_6]_4$ units depending on the compounds. A condensed type of unit is formed in the α-phase (Fig. 3(b)), whereas a lengthened type of unit, in the hp-phase (Fig. 3(d)). Tetrahedra are found in the β-phase and the hydrate, and are not directly linked with each other, but are located as if they constitute virtual $[MoO_4]_4$ z-shaped units. Figure 4 shows the detailed arrangements of the MoO_n polyhedra in the real and virtual $[MoO_n]_4$ z-shaped units observed in the four compounds [4,10,14,15]. The virtual unit in the β-phase (Fig. 4(c)) has dihedral symmetry and the two Mo atoms at both ends of the unit are located symmetrically against the two central Mo atoms (d_A : d_B = 4.19 : 4. 19) like those in the real condensed unit of the α-phase (d_A : d_B = 3.34 : 3.34). Thus, it is regarded as a virtual condensed type of unit. In the hydrate the two terminal Mo atoms are located not symmetrically against the central atoms (that is, the ratio (d_A : d_B = 4.62 : 4.21), and form a virtual lengthened type of unit (Fig. 4(a)). Thus, the hydrate has a coordination of the Mo atom similar to that in the β-phase, but the arrangements of the MoO_n polyhedra are similar to those in the hp-phase.

According to the above results the hydrate exhibits the coordinations of the metal cations similar to those of the β-phase, and has arrangements of MO_n (M=Co, Mo) polyhedra similar to those of the hp-phase. Such structural similarities allow hypothetical transformations of the hydrate into the β- and hp-phases by simple translational or rotational displacements of corresponding polyhedra, as shown in Fig. 5. Thus the real direct transformations can be achieved at lower temperatures.

Acknowledgements

The authors thank Dr. Masao Hashimoto for his valuable discussion. The work at Binghamton was supported by the National Science Foundation grant 0313963.

References

[1] A. P. Young, C. M. Schwartz, Science, 141 (1963) 348.

[2] A. W. Sleight, B. L. Chamberland, *Inorg. Chem.*, **7** (1968) 1672.

[3] M. Wiesmann, H. Ehrenberg, G. Wltschek, P. Zinn, H. Weitzel, H. Fuess, J. Magn. Magn. Mater. 150 (1995) L1.

[4] C. Livage, A. Hynaux, J. Marot, M. Nogues, G. Férey, J. Mater. Chem., 12 (2002) 1423.

[5] C. Mazzocchia, C. Aboumrad, C. Diagne, E. Tempesti, J. M. Herrmann, G. Thomas,

Catal Lett., 10 (1991) 181.

[6] J. Zou, G. L. Schrader, J. Catal., 161 (1996) 667.

[7] J. L. Brito, A. L. Barbosa, J. Catal., 171 (1997) 467.

[8] J. A. Rodriguez, S. Chaturvedi, J. Hanson, A. Albornoz, J. L. Brito, J. Phys. Chem. B 102 (1998) 1347.

[9] J. A. Rodriguez, S. Chaturvedi, J. Hanson, A. Albornoz, J. L. Brito, J. Phys. Chem. B 103 (1999) 770.

[10] G.. W. Smith, J. A. Ibers, Acta Cryst., 19 (1965) 269.

[11] P. Courtine, P. P. Cord, G. Pannetier, J. C. Daumas, R. Montarnal, Bull. Soc. Chim. Fr., (1968) 4816.

[12] F. Izumi, T. Ikeda, Mater. Sci. Forum 321-324 (2000) 198.

[13] F.E. Massoth, in: D.D. Eley, H. Pines, P.B. Weisz (Eds.), Advances in Catalysis, Vol. 27, 1978, p. 302.

[14] For the β-phase the atomic positions have not been presented yet. The separations among neighbor Mo atoms in this phase were evaluated using the atomic positions of α-$MnMoO_4$ [15], which is isostructural with β-$CoMoO_4$.

[15] S. C. Abrahams, J. M. Reddy, J. Chem. Phys. 43 (1965) 2533.

Table 1. Crystal data and structure refinement

Empirical formula	$CoMoO_4 \cdot 3/4H_2O$
Formula weight	232.38
Crystal system, space group	triclinic, $P\bar{1}$
a, b, c / Å	6.844(2), 6.933(2), 9.339(2)
α, β, γ / °	76.617(3), 84.188(7) 74.510(8)
V / Å^3, Z	415.1(2), 4
Temperature / K	293(2)
Calculated density / g cm^{-3}	3.758
μ / mm^{-1}	6.912
F(000)	436
Crystal dimensions / mm^3	0.19 × 0.04 × 0.03
θ range for data collection degrees	2.27 to 27.43
Limiting indices	$-8 \le h \le 8$, $-8 \le k \le 8$, $0 \le l \le 11$
Reflections collected	1569
Independent reflections	1569
Restraints, parameters	0, 77
$R1(F)$	0.0704
$wR2(F^2)$	0.1748 $w=1/[\sigma^2(Fo^2)+(0.1013P)^2+0.0000P]$ where $P=(Fo^2+2Fc^2)/3$
CSD no.	415282

Table 2. Atomic coordinates (×10000), equivalent isotropic displacements (Å^2×1000), and bond valence sums (BVS)

atom[a]	site	Occupancy	*x*	*y*	*z*	U_{eq}	BVS
Co1	2*i*	1.0	1543(3)	6464(3)	6992(2)	11 (1)	2.08
Co2	2*i*	1.0	1962(3)	8287(3)	9727(2)	9 (1)	2.14
Mo1	2*i*	1.0	59(2)	1935 (2)	6845(1)	11 (1)	5.91
Mo2	2*i*	1.0	2482 (2)	2943(2)	10522 (1)	9(1)	6.02
O1	2*i*	1.0	1447(14)	-726(14)	7476(11)	15(2)	1.96
O2	2*i*	1.0	1569(16)	3646(15)	6738(13)	21(2)	1.93
O3	2*i*	1.0	-826(16)	2211(15)	5125(13)	24(3)	2.01
O4	2*i*	1.0	-2102(14)	2633(14)	8019(11)	15(2)	1.80
O5	2*i*	1.0	2054(15)	5470(15)	9301(12)	15(2)	1.98
O6	2*i*	1.0	1284(15)	1361(14)	9831(12)	17(2)	2.12
O7	2*i*	1.0	1589(13)	3093(15)	12303(12)	18(2)	1.92
O8	2*i*	1.0	5048(13)	1891(15)	10582(12)	19(2)	2.08
$O9_{cw}$	2*i*	1.0	4685(16)	5952(17)	6310(12)	25(3)	0.33
$O10_{lw}$	2*i*	0.5	-4560(60)	-160(60)	5430(50)	81(13)	0.04

[a] see Fig. 3 for atomic numbering

Table 3. Selected interatomic distances (Å)

Co1 octahedron		Co2 octahedron		inter-cation	
Co1-O2	2.018(11)	Co2-O8	2.012(10)	Co1-Co2	3.169(3)
Co1-O3	2.026(11)	Co2-O4	2.054(10)	Co1-Mo1	3.583(2)
Co1-O1	2.088(10)	Co2-O5	2.069(10)	Co1-Mo1	3.629(3)
Co1-O5	2.139(11)	Co2-O6	2.087(10)	Co1-Mo1	3.684(3)
Co1-O7	2.139(10)	Co2-O1	2.092(10)	Co1-Mo2	3.418(2)
Co1-O9	2.141(11)	Co2-O6	2.177(10)	Co1-Mo2	3.620(2)
				Co2-Co2	3.159(2)
Mo1 tetrahedron		Mo2 tetrahedron		Co2-Mo1	3.338(2)
Mo1-O3	1.726(11)	Mo2-O8	1.714(10)	Co2-Mo1	3.342(2)
Mo1-O2	1.752(10)	Mo2-O7	1.732(10)	Co2-Mo2	3.413(2)
Mo1-O4	1.781(9)	Mo2-O6	1.781(10)	Co2-Mo2	3.532(2)
Mo1-O1	1.819(9)	Mo2-O5	1.822(10)	Co2-Mo2	3.588(2)
				Co2-Mo2	3.665(2)
				Mo1-Mo2	4.2328(19)
				Mo1-Mo2	4.3514(19)

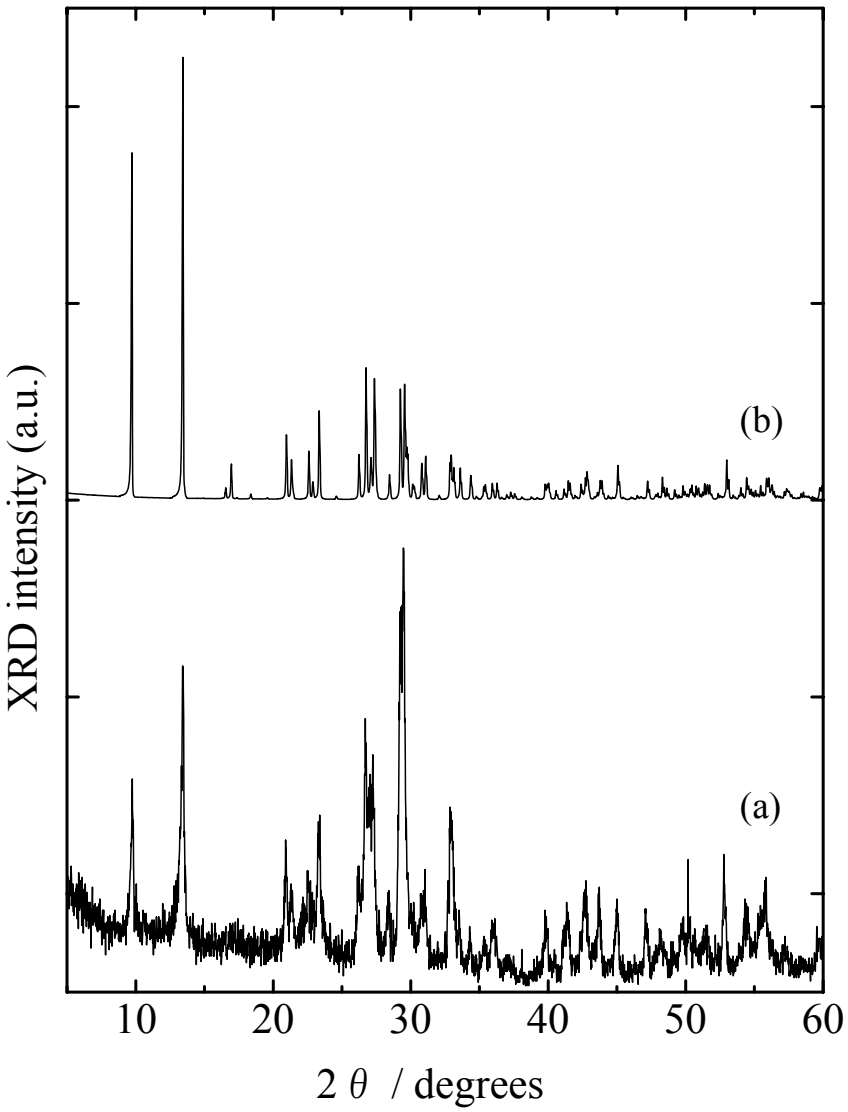

Figure 1. Powder XRD patterns of the hydrate: measured (a) and simulated (b).

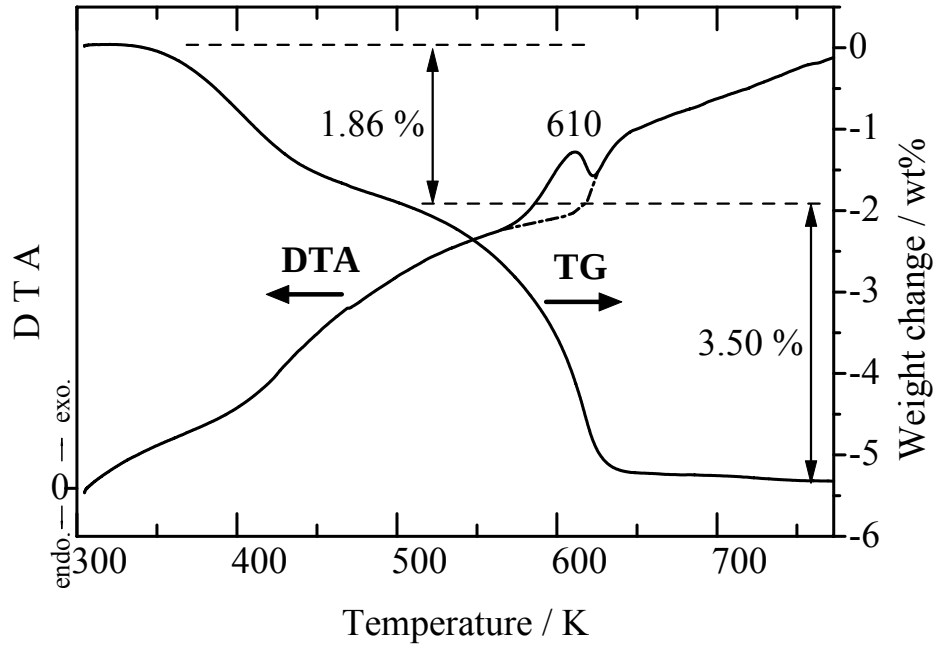

Figure 2. TG-DTA curves in N_2 of the hydrate.

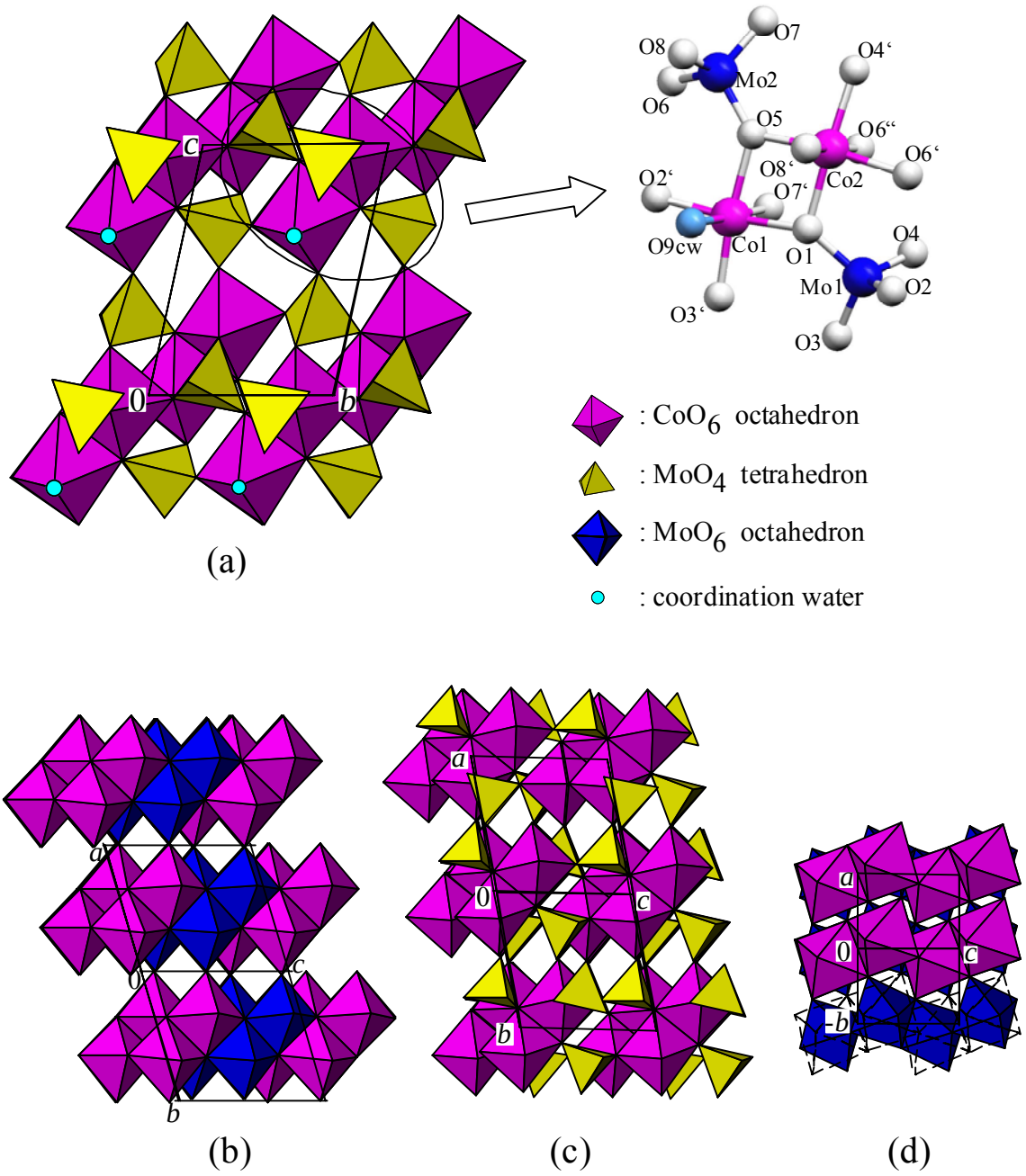

Figure 3. Polyhedral representations of the structures: hydrate (a), α-phase (b), β-phase (c), and hp-phase (d). Lattice water ($O10_{lw}$) of the hydrate is omitted for clarity.

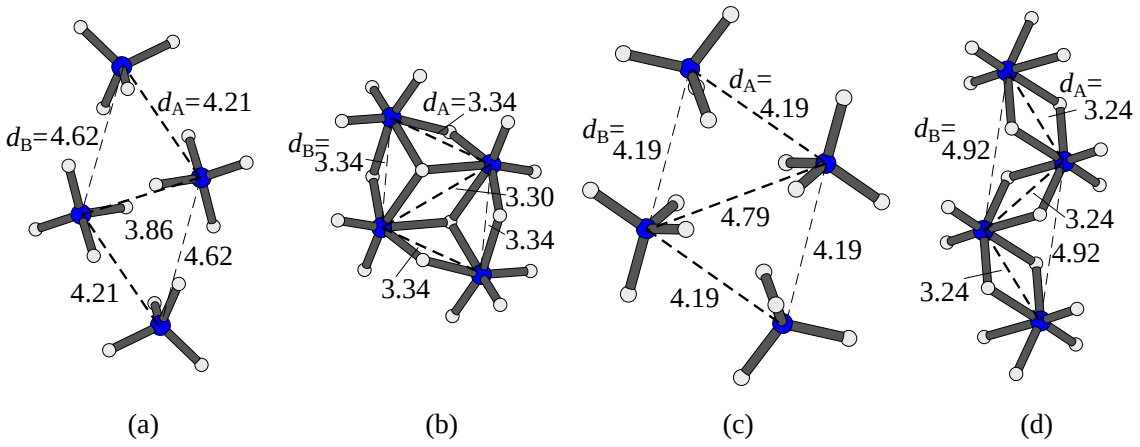

Fig. 4 by Eda et al.

Figure 4. Polyhedral configurations in the real and virtual z-shaped $[MoO_n]_4$ units: hydrate (a), α-phase (b), β-phase [13] (c), and hp-phase (d). Separations among neighboring Mo atoms are presented in Å..

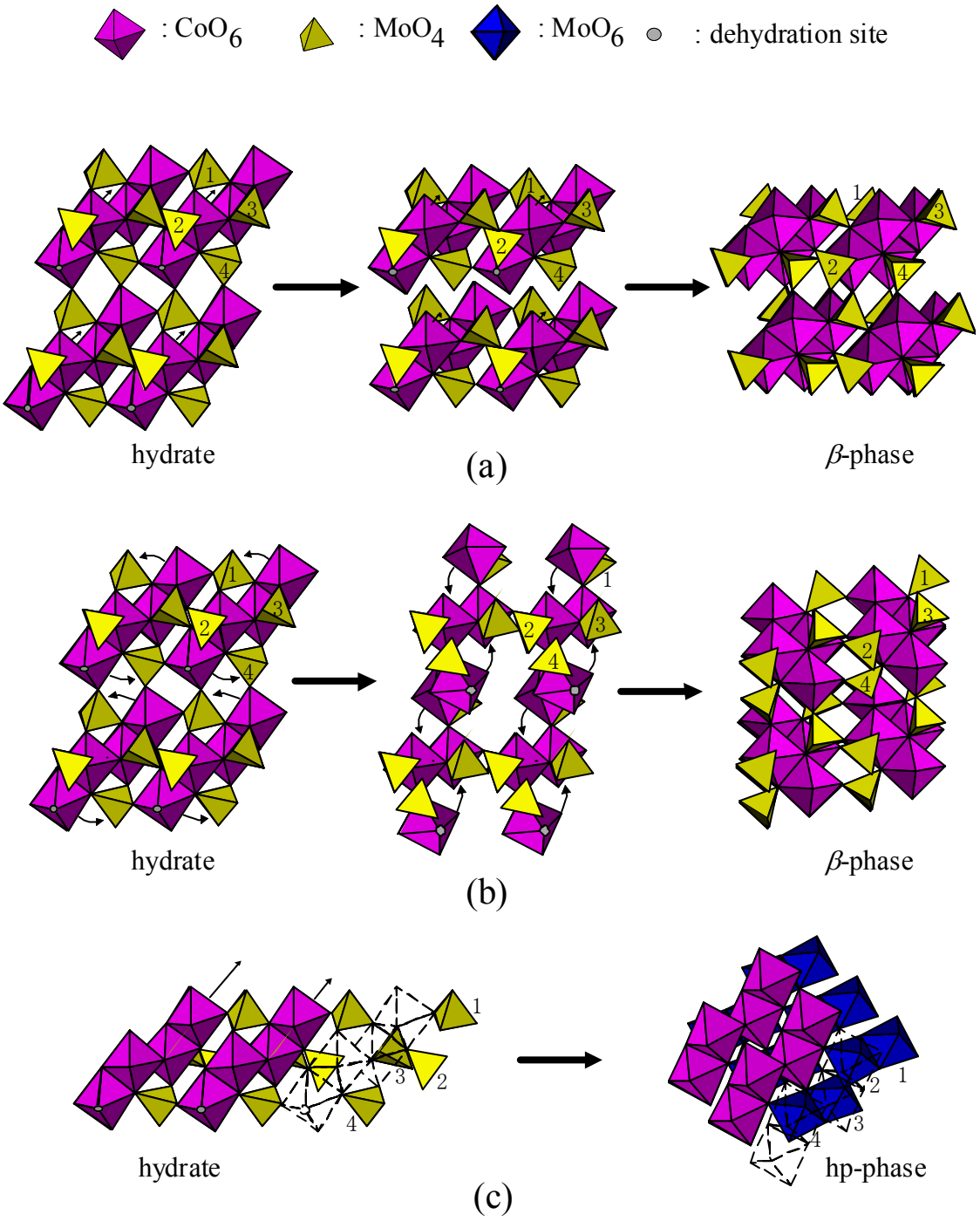

Figure 5. Hypothetical mechanisms of the structural transformations: from hydrate to *β*-phase mainly with translational displacements (a), from hydrate to *β*-phase mainly with rotational displacements (b), and from hydrate to hp-phase mainly with translational displacements (c).